Supplementary Materials

Growth redox conditions and interface effects govern polarization switching speed, retention and reliability in epitaxial $Hf_{0.5}Zr_{0.5}O_2$ thin films

Xueliang Lyu[#], Faizan Ali[#], Florencio Sánchez, Ignasi Fina

Institut de Ciència de Materials de Barcelona (ICMAB-CSIC), Carrer dels Til.lers, Cerdanyola del Vallès 08193 Spain.
[#]Authors contributed equally.

Correspondence to: Dr. Florencio Sánchez, Dr. Ignasi Fina, Institut de Ciència de Materials de Barcelona (ICMAB-CSIC), Campus UAB, Barcelona 08193, Spain. E-mail: fsanchez@icmab.es; ifina@icmab.es

Table S1. Summary of the Nucleation-Limited Switching (NLS) model fitting parameters for $Hf_{0.5}Zr_{0.5}O_2$ thin films deposited on STO(001) under a pure O_2 atmosphere.

Thickness (nm)	Fitting range (ns)	P_r (μC/cm^2)	t_1 (ns)	Confidence intervals (μC/cm^2)	Goodness-of-fit values (R^2)
4.5	25 -10^6	6.3	39.8	6.12-6.48	0.605
5.7	25 -10^6	13.2	45.7	12.97-13.43	0.973
6.8	25 -10^6	18.0	100	17.90-18.10	0.994
7.9	25 -10^6	15.7	126	15.46-15.94	0.980
9.0	25 -10^6	16.0	97.7	15.9-16.1	0.996
13.6	25 -10^6	4.9	100	4.89-4.91	0.999
18.1	25 -10^6	1.8	87.1	1.77-1.83	0.996

Table S2. Summary of the Nucleation-Limited Switching (NLS) model fitting parameters for $Hf_{0.5}Zr_{0.5}O_2$ thin films deposited on STO(110) under a pure O_2 atmosphere.

Thickness (nm)	Fitting range (ns)	P_r (μC/cm^2)	t_1(ns)	Confidence intervals (μC/cm^2)	Goodness-of-fit values (R^2)
4.5	25 -10^6	9.2	48.9	9.08-9.32	0.987
5.7	25 -10^6	12.6	125.9	12.33-12.87	0.987
6.8	25 -10^6	22.1	91.2	21.83-22.37	0.991
7.9	25 -10^6	17.6	93.3	17.39-17.81	0.989
9.0	25 -10^6	15.1	87.1	14.81-15.39	0.981
13.6	25 -10^6	3.3	63.1	3.18-3.42	0.890
18.1	25 -10^6	2.9	43.7	2.80-3.00	0.790

Table S3. Summary of the Nucleation-Limited Switching (NLS) model fitting parameters for $Hf_{0.5}Zr_{0.5}O_2$ thin films deposited on STO(110) under a mixture O_2/Ar atmosphere.

Thickness (nm)	Fitting range (ns)	P_r (μC/cm^2)	t_1(ns)	Confidence intervals (μC/cm^2)	Goodness-of-fit values (R^2)
3.6	25 -10^6	6.2	43.7	6.17-6.23	0.992
4.5	25 -10^6	16.8	91.2	16.76-16.84	0999
5.4	25 -10^6	22.1	91.2	21.82-22.38	0.993
6.3	25 -10^6	17.5	91.2	16.74-18.24	0.928
7.2	25 -10^6	34.5	132.0	33.38-35.62	0.905
10.8	25 -10^6	9.7	74.1	9.22-10.18	0.803
14.4	25 -10^6	4.0	91.2	3.80-4.20	0.737

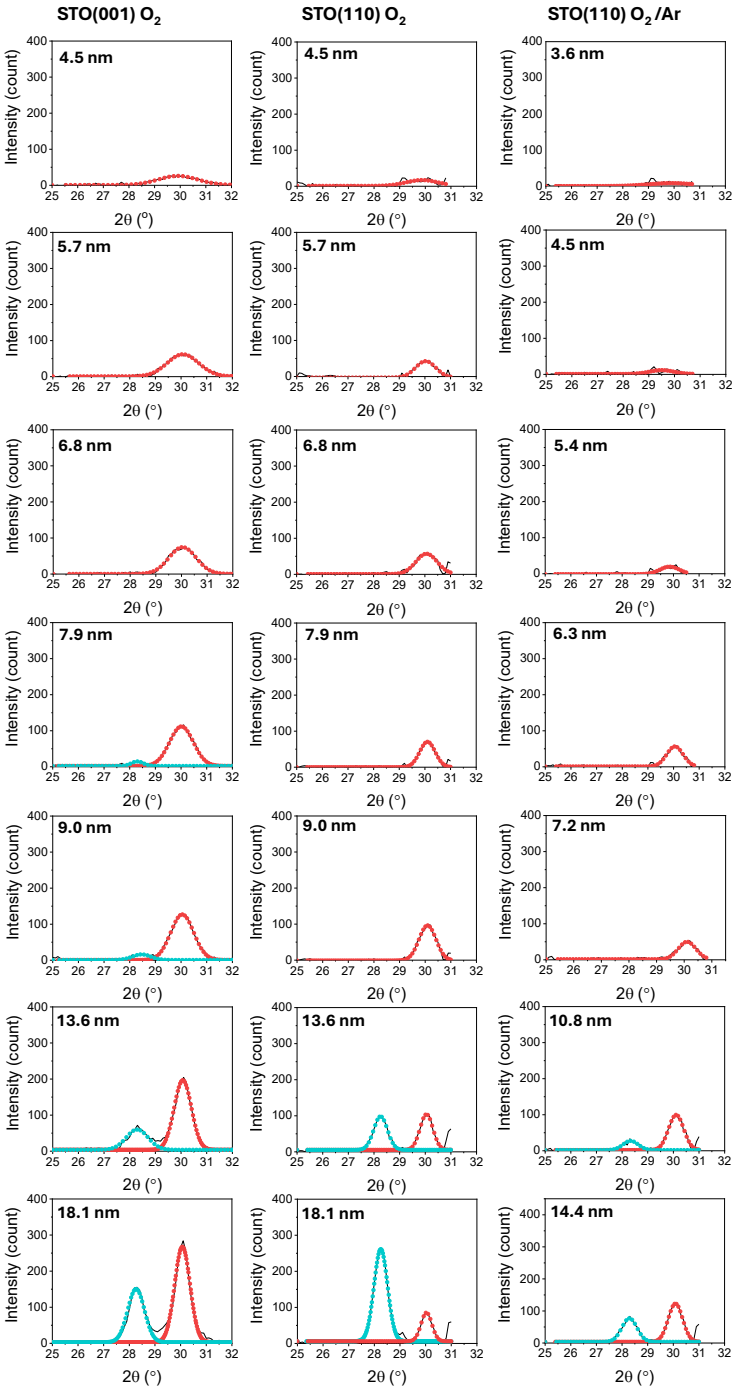

Figure S1. 2θ patterns obtained by χ-integration of the χ–2θ maps for HZO films grown on (left) STO(001) O_2, (middle) STO(110) O_2, and (right) STO(110) O_2/Ar substrates with different thicknesses. The orthorhombic (o) and monoclinic (m) phase contributions are indicated by red and cyan curves, respectively.

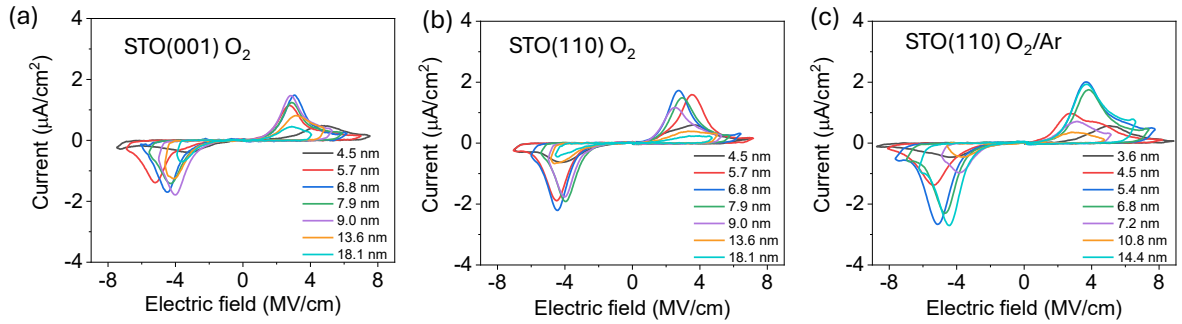

Figure S2. Current–electric field (I–E) curves corresponding to the ferroelectric polarization loops shown in Figure 2 for (a) STO(001) O_2, (b) STO(110) O_2, and (c) STO(110) O_2/Ar.

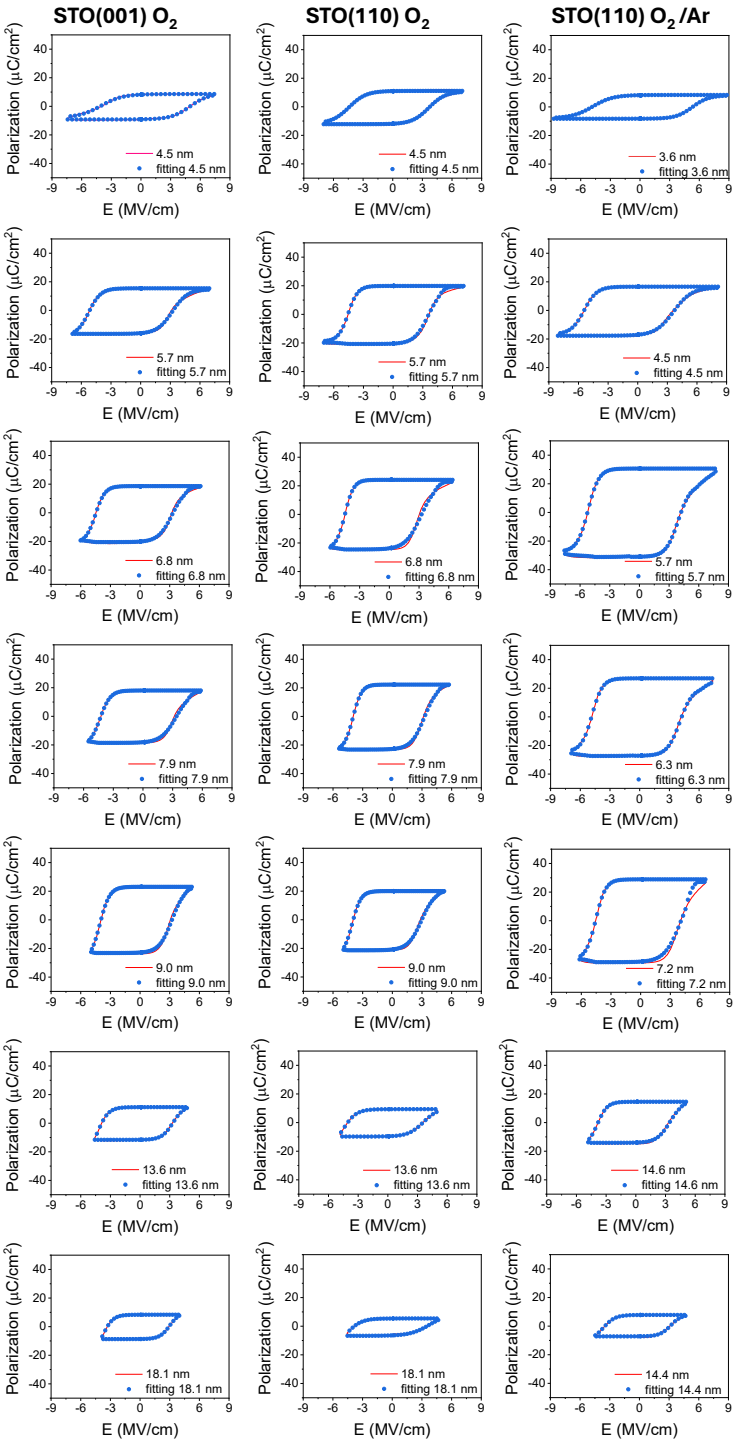

Figure S3. Representative fits of the polarization–electric field (P–E) hysteresis loops using the tangent model for the different samples and thicknesses. Experimental data are shown as symbols, while the solid lines correspond to the fitted curves.

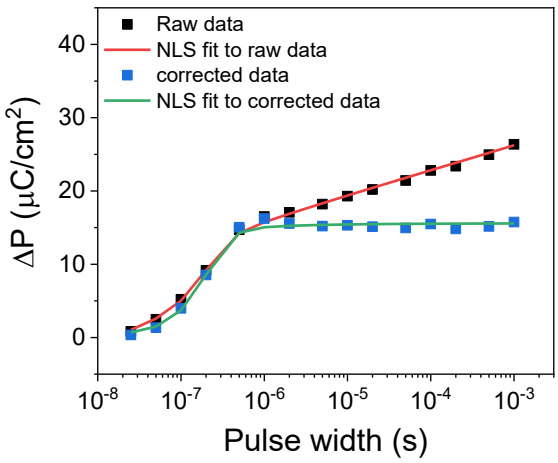

Figure S4. Comparison of experimental switched polarization (ΔP) versus writing pulse width for an HZO film with thickness 6.8 nm, grown on STO (001) under O_2, shown before and after subtraction of the fitted residual leakage contribution.

To accurately extract the switched polarization (ΔP) of the $Hf_{0.5}Zr_{0.5}O_2$ capacitors, we applied a fitting procedure that accounts for the residual leakage current contribution, which is not completely removed by the conventional Positive-Up Negative-Down (PUND) method. The experimental ΔP was fitted using the Nucleation-Limited Switching (NLS) model, modified to include a logarithmic leakage term:

$$\Delta P = 2P_r \int_{-\infty}^{+\infty} \left[1 - e^{-\left(\frac{t}{\tau}\right)^n}\right] F(\log \tau) \times d(\log \tau) + Q.\log(\tau_w) \qquad (1)$$

where n is the effective dimension (fixed at n =2), τ is the characteristic switching time, and F(log τ) is the Lorentzian distribution for the logarithm of switching time. The Lorentzian distribution can be expressed as:

$$F(\log\tau) = \frac{A}{\pi}\left[\frac{w}{(\log\tau - \log t_1)^2 + w^2}\right] \quad (2)$$

where A is a normalization constant, w is the full width at half maximum (FWHM), and log t_1 is the central value of the Lorentzian distribution for the logarithm of switching time. The additional $Q.\log(\tau_w)$ term represents the phenomenological residual leakage current contribution, where Q is a constant.

The corrected switched polarization was obtained by subtracting the fitted $Q.\log(\tau_w)$ term from the raw ΔP data. This term captures the residual logarithmic increase in polarization at longer writing times due to coexisting electronic and ionic leakage mechanisms, which cause hysteretic conductivity (resistive switching) in hafnia-based films. After subtraction, the corrected ΔP curves saturate as expected, confirming that the remaining signal corresponds to true ferroelectric switching. Figure S4 compares the experimental ΔP data before and after leakage subtraction for an $Hf_{0.5}Zr_{0.5}O_2$ sample deposited at 0.1 mbar P_{O2} and on STO(001).

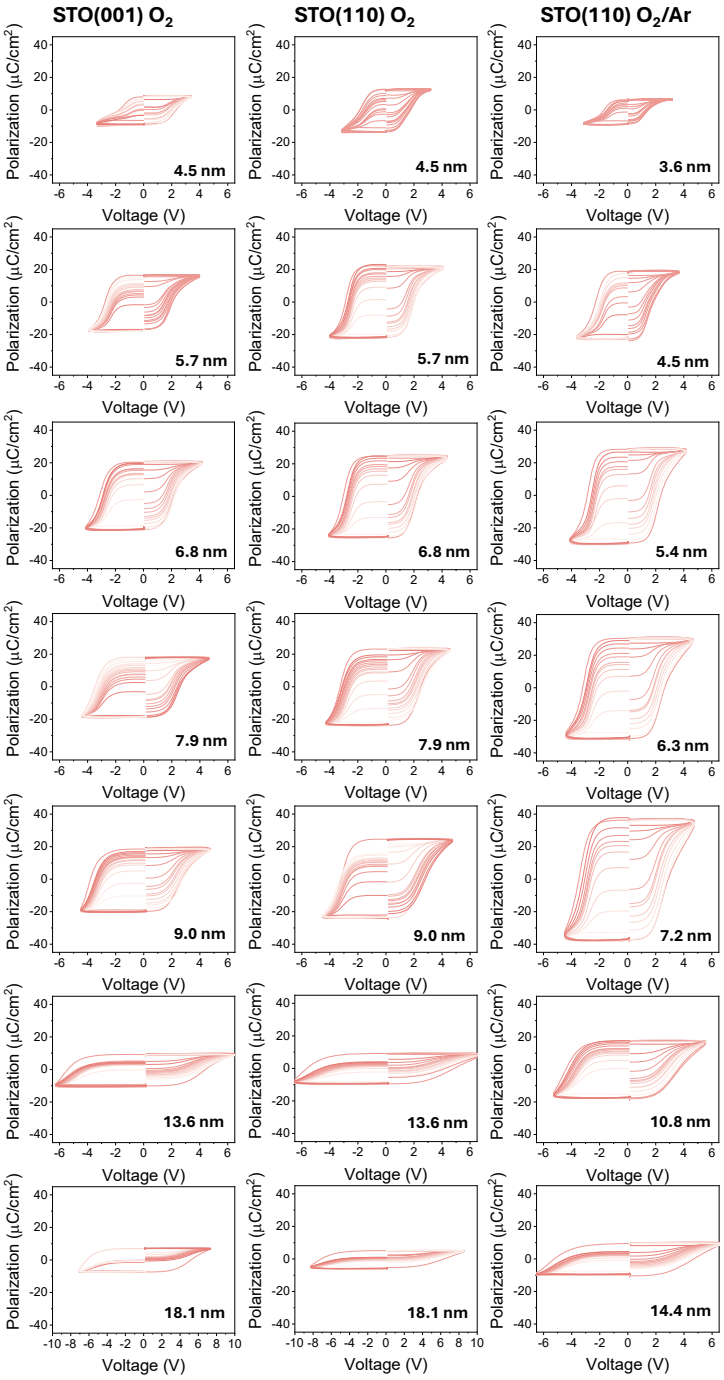

Figure S5. PUND reading loops measured for increasing writing pulse widths used in the switching spectroscopy experiments corresponding to Figure 3 for STO(001) O_2 (left), STO(110) O_2 (middle), and STO(110) O_2/Ar (right).

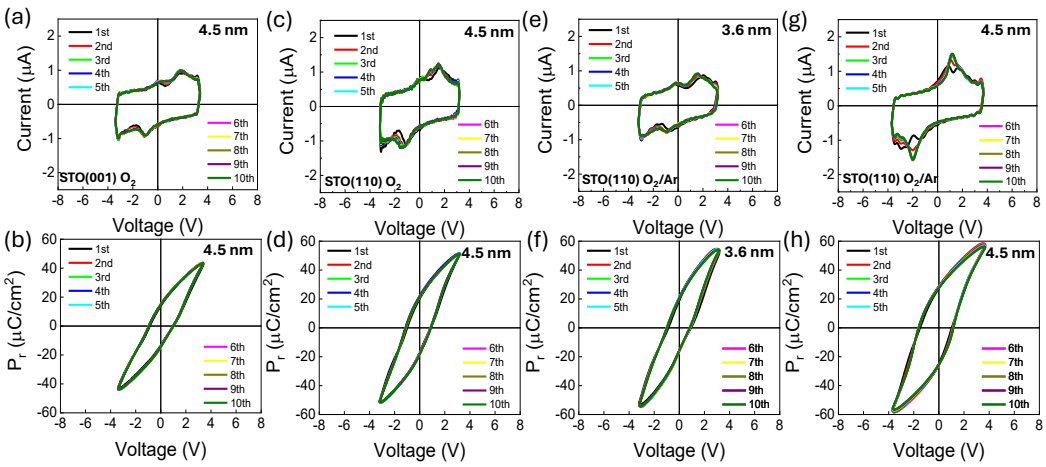

Figure S6. I–V and P–V loops measured after several cycles of HZO samples grown on (a) and (b) STO(001) O_2 with a thickness of 4.5 nm; (c) and (d) STO(110) O_2 with a thickness of 4.5 nm; (e) and (f) STO(110)O_2/Ar with a thickness of 3.6 nm; (g) and (h) STO(110)/Ar with a thickness of 4.5 nm.

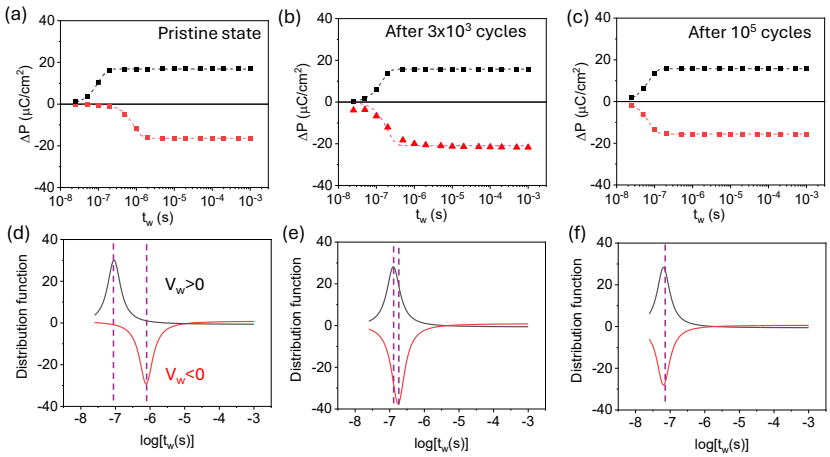

Figure S7. Switching measurements of HZO film with a thickness of 4.5 nm, grown on STO(110) under O_2/Ar atmosphere. (a–c) Switched polarization ΔP as a function of writing pulse width t_w together with the NLS fits for (a) the pristine state, (b) after 3×10^3 switching cycles, and (c) after 1×10^5 cycles. (d–f) Corresponding Lorentzian switching-time distributions extracted from the NLS analysis for the same cycling states.

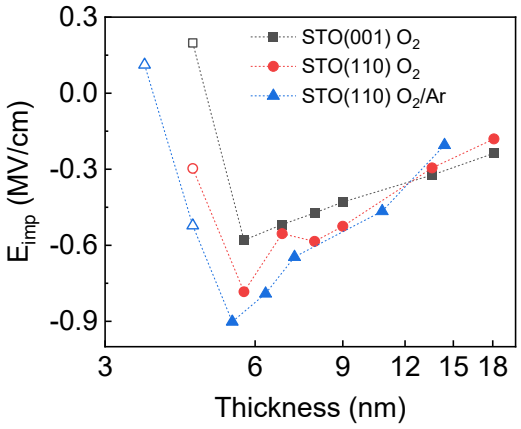

Figure S8. Thickness dependence of the imprint electric field (E_{imp}) of $Hf_{0.5}Zr_{0.5}O_2$ thin films deposited on (001) or (110) oriented STO substrates and under varying growth atmospheres. The three series correspond to films grown on (001)-oriented STO in pure O_2 (black squares), (110)-oriented STO in pure O_2 (red circles), and (110)-oriented STO in an O_2/Ar mixed ambient (blue triangles).

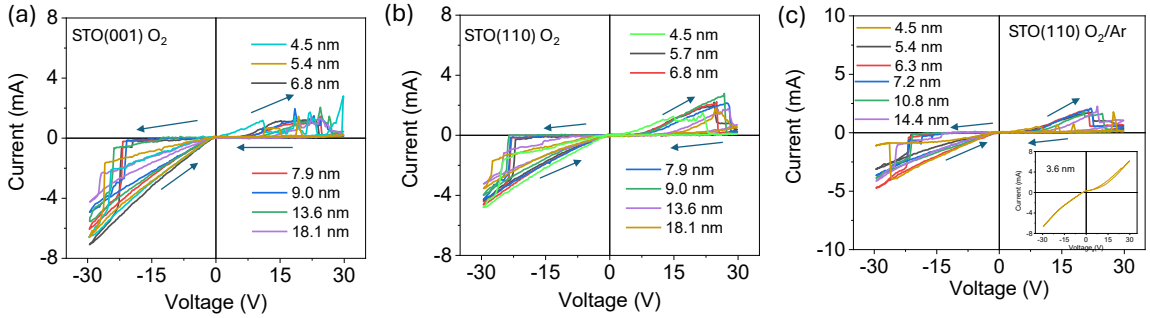

Figure S9. Current–electric field (I–V) curves measured for films with different thicknesses of (a) STO(001) O_2, (b) STO(110) O_2, and (c) STO(110) O_2/Ar. Inset of panel (c) corresponds to a 3.6 nm thick HZO film, where dielectric breakdown was not detected in the used measurement conditions.

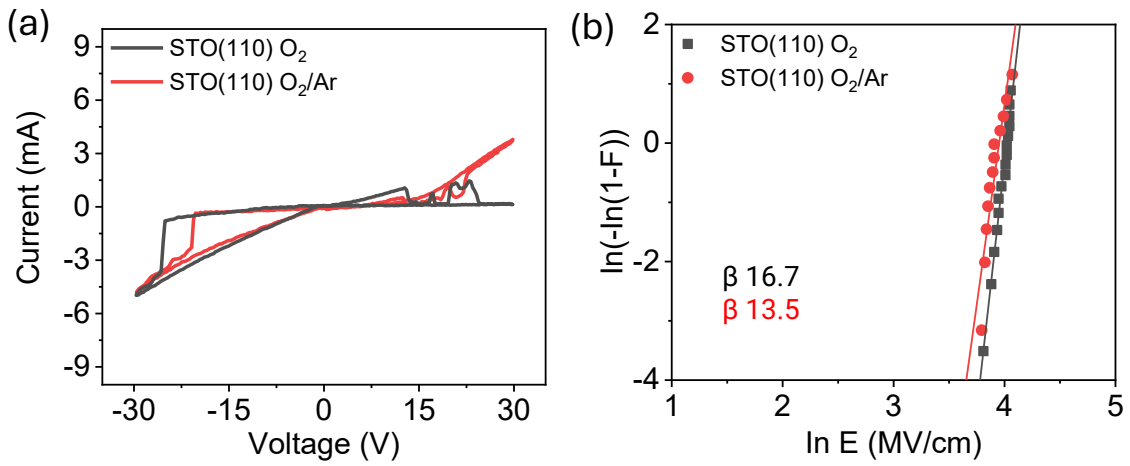

Figure S10. (a) Current-voltage (I-V) curves collected at high voltage and (b) Weibull statistical distributions of the breakdown electric field (E_{BD}) of 4.5 nm thick $Hf_{0.5}Zr_{0.5}O_2$ films deposited on STO(110) under pure O_2 and a mixture of O_2/Ar atmosphere.

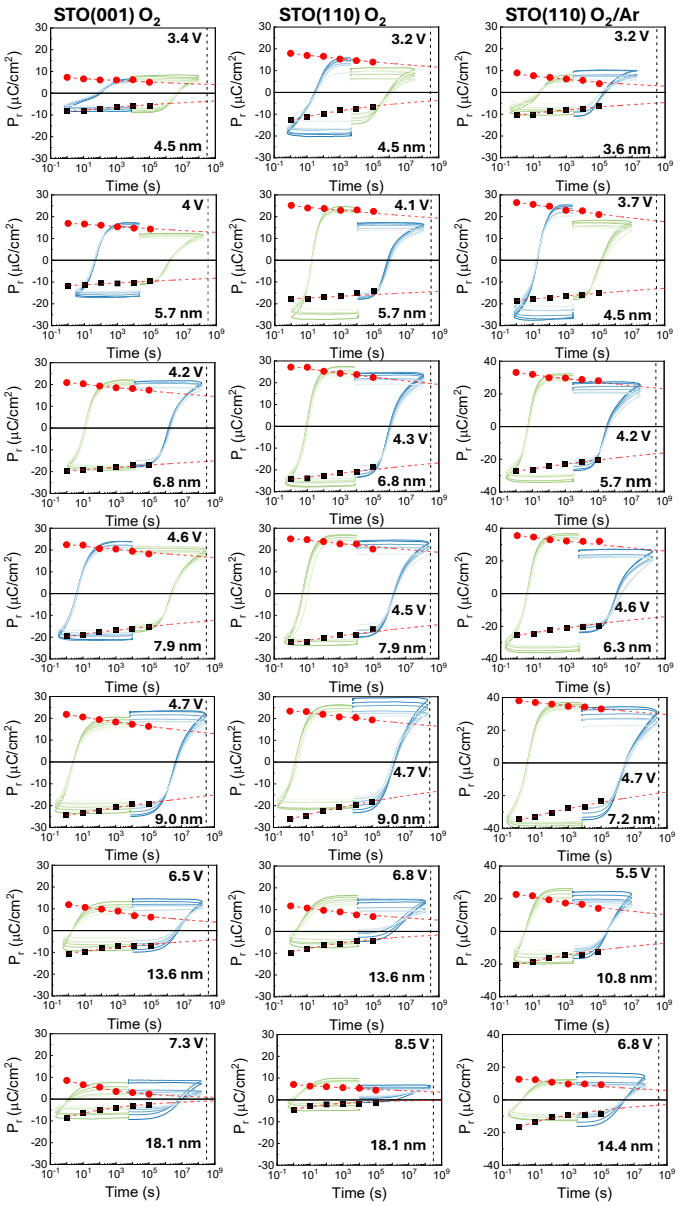

Figure S11. Retention behavior of the remanent polarization (P_r) as a function of delay time for the three series, across increasing film thickness (row, top to bottom). In each panel, the black squares and red circles denote the P_r values extracted from the positive and negative switching states, respectively. The overlaid blue and green loops show the corresponding PUND hysteresis loops from which P_r values were obtained. The applied voltage and film thickness for each sample are indicated in each panel, respectively.

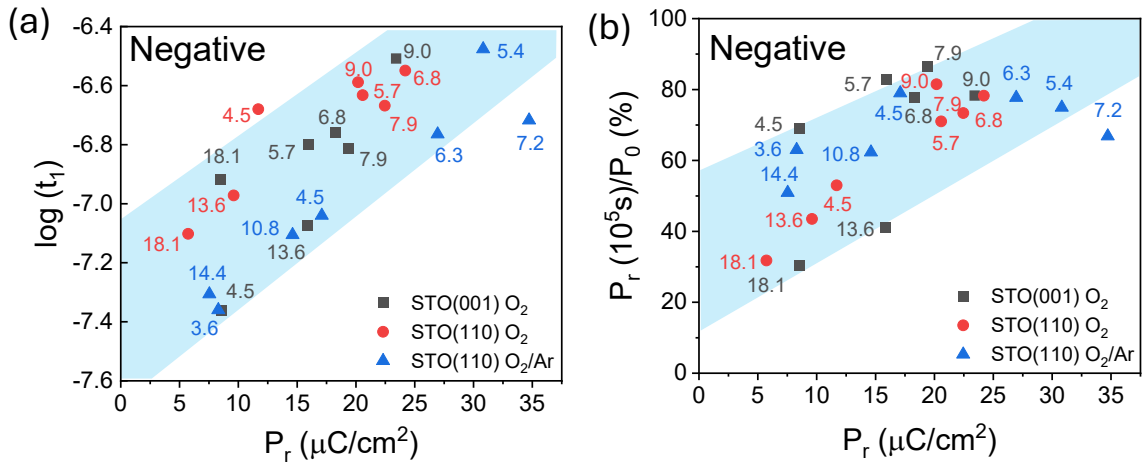

Figure S12. (a) Characteristic switching time and (b) normalized polarization retention $Pr(10^5s)/P_0$ (%) as a function of polarization. Numbers indicate film thickness in nm.